

Cooperative Gradient Coding for Collaborative Federated Learning

Shudi Weng, Chengxi Li, Ming Xiao, Mikael Skoglund

School of Electrical Engineering and Computer Science

KTH Royal Institute of Technology

Stockholm, Sweden

{shudiw,chengxli,mingx,skoglund}@kth.se

Abstract

We investigate federated learning (FL) in the presence of stragglers, with emphasis on wireless scenarios where the power-constrained edge devices collaboratively train a global model on their local datasets and transmit local model updates through fading channels. To tackle stragglers resulting from link disruptions without requiring accurate prior information on connectivity or dataset sharing, we propose a gradient coding (GC) scheme based on cooperative communication, which remains applicable to general collaborative FL. Furthermore, we conduct an outage analysis of the proposed scheme, based on which we conduct the convergence analysis. The simulation results reveal the superiority of the proposed strategy in the presence of stragglers, especially under imbalanced data distribution.

Index Terms

Collaborative federated learning, gradient coding, cooperative communication, outage, convergence

I. INTRODUCTION

Federated learning (FL) is a burgeoning domain within distributed optimization in e.g., Internet-of-Things (IoT) and cloud computing applications. FL employs a privacy-preserving framework where both data collection and model training are pushed to numerous edge devices [2], [3]. These edge devices collaboratively train a global model by sharing local models/model updates via wireless links, thereby bypassing the necessity of transmitting raw data wirelessly [4], [5].

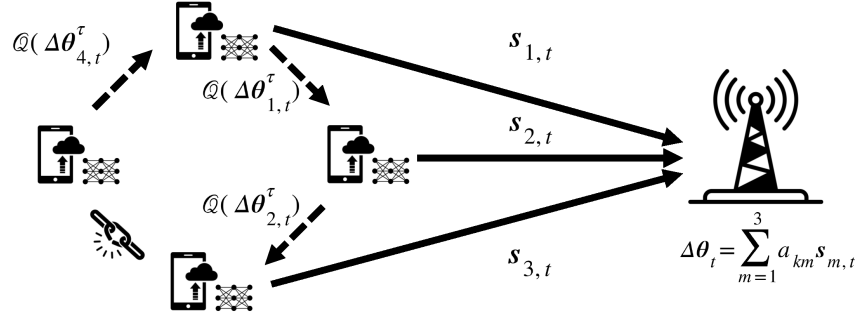


Fig. 1: An illustration of the proposed method in the r -th round. In this scenario, we set $M = 4$, $s = 1$, with 1 straggler occurring in stage (a).

However, limited by communication resources such as bandwidth and power constraints, edge devices may suffer link disruption (due to e.g., fading, interference) and fail to upload their local models/model updates [6], [7]. Such devices refer to communication stragglers. [9] explores the impact of partial participation induced by communication stragglers on FL performance, highlighting its potential to significantly degrade performance. Furthermore, the authors propose to mitigate the imbalance of partial participation by optimizing resource allocation under outage and delay constraints. In essence, this method overlooks contributions from stragglers. However, the existence of stragglers can induce a large generalization gap in model training, especially for the heterogeneous data distribution across devices [10]. Different from [9], [10] introduces a collaborative relaying strategy in FL to ensure that the local models of the poorly connected devices are conveyed to the central parameter server (PS) with the help of their neighbors. To ensure unbiased recovery of the global model over the intermittent network, collaboration weights among devices rely on precise prior knowledge of full connectivity information. However, the acquisition of such precise prior knowledge increases the complexity, particularly in dynamic environments. Considering that FL prohibits raw data sharing, [11] claims the necessity of new GC schemes in wireless FL to tackle stragglers. [12] extends gradient coding (GC) from distributed learning (DL) to FL by sharing the coded datasets across devices such that devices cannot discern the datasets of other devices due to the added randomness. However, for large datasets and a massive number of devices, the transmission of coded datasets takes excessive power and time. To overcome the limitations of the existing methods this work proposes a new GC method cooperative communication based for FL.

Our main contributions are summarized as follows.

- We propose a straggler-resilient GC scheme based on cooperative communication, without requiring precise prior connectivity information and data sharing. The proposed method remains applicable to general collaborative FL not necessarily connected via wireless links.
- We conduct an outage analysis of the proposed zero-tolerance strategy over the intermittent network in which the global model updates either can be recovered perfectly or cannot be recovered at all. We further specifying the failure probability of the proposed scheme each round and provide a novel convergence analysis in which the number of local iterations per round varies depending on the network connectivity.
- We verify the proposed method by simulations. The results show that our proposed method attains better learning performance than the baseline methods and demonstrates excellent stragglers-handling ability.

II. STATE OF ART

A. Federated Learning with Quantized Transmission

Consider a FL network consisting of M edge devices and a PS to jointly solve the following optimization problem:

$$\min_{\boldsymbol{\theta} \in \mathbb{R}^d} \left[F(\boldsymbol{\theta}) := \sum_{m=1}^M p_m F_m(\boldsymbol{\theta}) \right], \quad (1)$$

where $\boldsymbol{\theta} \in \mathbb{R}^d$ denotes the global model, $p_m = n_m/n$ denotes the relative sample size at device $m \in [M]$, $F_m(\boldsymbol{\theta}) = \frac{1}{n_m} \sum_{\xi \in \mathcal{D}_m} f_m(\boldsymbol{\theta}, \xi)$ is the local objective function at device $m \in [M]$. Here, f_m is the loss function defined by the learning model, ξ represents a data sample from local dataset \mathcal{D}_i , n_m is the number of data samples on device m and n is the total number of data samples across all devices.

To solve (1), the FedAvg algorithm [13] is widely used. In FedAvg, the following steps are executed at each round $t \in [T]$, where T is the total number of communication rounds.

1) *Broadcasting*: At the beginning of each communication round t , the PS assigns the global model $\boldsymbol{\theta}_{t-1}$ to all devices.

2) *Training*: Device m receives the global model and sets $\boldsymbol{\theta}_{m,t}^0 = \boldsymbol{\theta}_{t-1}$, and performs τ -step stochastic gradient descent (SGD). At iteration $i \in [\tau]$, the local model is updated as

$$\boldsymbol{\theta}_{m,t}^i \leftarrow \boldsymbol{\theta}_{m,t}^{i-1} - \eta \nabla F_m(\boldsymbol{\theta}_{m,t}^{i-1}, \xi_{m,t}^i), \quad (2)$$

where $\eta > 0$ is the learning rate, and the $\nabla F_m(\boldsymbol{\theta}_{m,t}^{i-1}, \xi_{m,t}^i)$ is the stochastic gradient computed on a training data sample $\xi_{m,t}^i$ at i -th iteration of t -th round on device m .

3) *Transmission and Aggregation*: Afterward, the local model updates $\Delta\boldsymbol{\theta}_{m,t}^\tau$ s are quantized before transmission employing stochastic quantization (SQ) at devices [6], [9]. For simplicity of notation, let u_l denote the l -th entry in $\Delta\boldsymbol{\theta}_{m,t}^\tau \in \mathbb{R}^d$. Assume that for $\forall l \in [d]$, the absolute value of the l -th entry u_l in $\Delta\boldsymbol{\theta}_{m,t}^\tau \in \mathbb{R}^d$ is bounded, i.e., $|u_l| \in [\underline{u}_l, \overline{u}_l]$. The number of quantization levels is set to 2^B , where B is the number of quantization bits. We denote $\{c_0, c_1, \dots, c_{2^B-1}\}$ as knobs uniformly distributed in $[\underline{u}_l, \overline{u}_l]$, that is,

$$c_q = \underline{u}_l + q \times \frac{\overline{u}_l - \underline{u}_l}{2^B - 1}, \quad (3)$$

where $q = 0, \dots, 2^B - 1$. The parameter u_l whose absolute value $|u_l|$ falls in $[c_q, c_{q+1})$ is quantized by

$$\mathcal{Q}(u_l) = \begin{cases} \text{sign}(u_l) \cdot c_q, & \text{w.p. } \frac{c_{q+1} - |u_l|}{c_{q+1} - c_q} \\ \text{sign}(u_l) \cdot c_{q+1}, & \text{w.p. } \frac{|u_l| - c_q}{c_{q+1} - c_q}. \end{cases} \quad (4)$$

Vector SQ (VSQ) is performed element-wise on $\Delta\boldsymbol{\theta}_{m,t}^\tau \in \mathbb{R}^d$ and $\mathcal{Q}(\Delta\boldsymbol{\theta}_{m,t}^\tau)$ is represented by $dB + \mu$ bits, where μ is the number of bits to represent $\frac{\Delta\boldsymbol{\theta}_{m,t}^\tau}{\overline{\Delta\boldsymbol{\theta}_{m,t}^\tau}}$ and $\text{sign}(\Delta\boldsymbol{\theta}_{m,t}^\tau)$. For simplicity, we assume the same number of quantization bits B for all devices. For full participation of devices, PS performs aggregation and updates the global model as

$$\boldsymbol{\theta}_t \leftarrow \boldsymbol{\theta}_{t-1} + \sum_{m=1}^M p_m \mathcal{Q}(\Delta\boldsymbol{\theta}_{m,t}^\tau). \quad (5)$$

B. Cooperative Communication and Transmission Outage

Our cooperative communication system refers to [14]. There are two communication stages: (a) device-to-device communication and (b) device-to-PS communication respectively. The individual links in each stage are assumed to be independent and identically distributed (i.i.d.) block fading channels. In all transmissions, device $m \in [M]$ transmits its message with systematic Gaussian codewords at rate R under signal-to-noise ratio (SNR) SNR_x in stage (x), where $x \in \{a, b\}$. Let $h_{m,m'}^x$ be the fading channel gain from device m to $m' \in \{\mathcal{M}_x\}$ in stage (x), where $\mathcal{M}_a = [M] \setminus m$ and $\mathcal{M}_b = \{\text{PS}\}$. An outage occurs when the channel capacity is less than the transmission rate, i.e., when $C < R$, where $C = \frac{1}{2} \log(1 + |h_{m,m'}^x|^2 \text{SNR}_x)$. Or equivalently, when $|h_{m,m'}^x|^2 < g_x$, where $g_x = \frac{2^{2R} - 1}{\text{SNR}_x}$. Assume Rayleigh fading, i.e., $|h_{m,m'}^x|$ follows Rayleigh distribution characterized by β_x , the outage probability P_e^x per transmission in stage (x) is given by $P_e^x = 1 - e^{-g_x/2\sigma_x^2}$. If PS is relatively far from devices, $\beta_b < \beta_a$ due to path loss.

C. Gradient Coding in Distributed Learning

In [15], to address computational stragglers in DL among M devices, GC is proposed to assign devices redundant datasets according to a cyclic allocation matrix $\mathbf{B}_{\text{cyc}} \in \mathbb{R}^{M \times M}$:

$$\mathbf{B}_{\text{cyc}} = \begin{bmatrix} \overbrace{\star \ \dots \ \star \ \star}^{s+1} & 0 & 0 & \dots & 0 \\ 0 & \star & \dots & \star & \star & 0 & \dots & 0 \\ \vdots & \ddots & \ddots & \ddots & \ddots & \ddots & \ddots & \vdots \\ 0 & \dots & 0 & \star & \star & \dots & \star & 0 \\ 0 & \dots & 0 & 0 & \star & \dots & \dots & \star \\ \star & 0 & \dots & 0 & 0 & \star & \dots & \star \\ \vdots & \ddots & \ddots & \ddots & \ddots & \ddots & \ddots & \vdots \\ \star & \dots & \star & 0 & 0 & \dots & 0 & \star \end{bmatrix}. \quad (6)$$

The combination matrix $\mathbf{A} \in \mathbb{R}^{f \times M}$, where $f = \binom{M}{s}$ at PS is designed such that $\forall k \in [f] : \mathbf{a}_k \mathbf{B}_{\text{cyc}} = \mathbb{1}_{1 \times M}$, where \mathbf{a}_k represents the k -th row vector of \mathbf{A} and $\mathbb{1}_{1 \times M}$ represents an all-one row vector of size M . After computing gradients over all allocated datasets in each round, each non-straggler device sends a weighted sum of these gradients to PS. Then PS detects the corresponding straggler pattern $\mathbf{a}_{k'}$, wherein the positions of zeros cover the indices of stragglers, and computes the global gradient by combining the received weighted sum according to $\mathbf{a}_{k'}$. The algorithm to generate \mathbf{A} and \mathbf{B}_{cyc} is given in [15]. The GC scheme is robust to any s stragglers in DL, however, it is not directly applicable within FL due to the prohibition of sharing raw datasets.

III. THE PROPOSED METHOD

Inspired by [15], we propose a cooperative GC scheme illustrated in Fig. 1 to address stragglers in FL. Our system setup consists of a group of M devices and a relatively distant PS, the same as in FedAvg described in II-A. All devices and PS deploy the same systematic Gaussian codebook. Setting preliminary communication rounds T , here, we describe the learning process at the t -th communication round.

1) *Broadcasting*: Different from FedAvg, in our design, whether to broadcast the global model at the beginning of the t -th round depends on whether PS was updated at the previous $t - 1$ -th round. If updated, PS broadcasts the latest global model θ_{t-1} to all edge devices. Otherwise, PS

foregoes broadcasting the global model. For simplicity, the downlink channel is assumed to be error-free.

2) *Training*: If PS broadcasts θ_{t-1} , the edge devices set $\theta_{m,t}^0 = \theta_{t-1}$ and performs t -th round of local training as in Eq. 2. Otherwise, the devices initialize with its newest local model by setting $\theta_{m,t}^0 = \theta_{m,t-1}^\tau$ and perform local training.

3) *Transmission and Aggregation*: After completing the local training, device m quantizes its local model update to $\mathcal{Q}(\Delta\theta_{m,t}^\tau)$ utilizing SQ techniques in II-A. Subsequently, the following two communication stages are carried out.

(a) *Device-to-device Communication*: First, device m encodes its quantized local model update $\mathcal{Q}(\Delta\theta_{m,t}^\tau) \in \mathbb{R}^d$ to message $I_{m,t}^a$ with the systematic Gaussian codebook. Let $b_{mm'}$ denote the (m, m') -th entry in B_{cyc} . Device m' , a neighbor of device m corresponding to $b_{mm'} \neq 0$ for $m' \neq m$, transmits $I_{m',t}^a$ to device m with SNR_a , then device m decode $\mathcal{Q}(\Delta\theta_{m',t}^\tau)$ s from the received $I_{m',t}^a$ s. The link from device m' to device m may suffer disruption w.p. P_e^a given in II-B. If device m recovers all updates from its s neighbors, it computes the partial sum of neighbors' local model updates as

$$\mathbf{s}_{m,t} = \sum_{n=1}^M b_{mm'} p_{m'} \mathcal{Q}(\Delta\theta_{m',t}^\tau). \quad (7)$$

If device m fails to receive all updates from its s neighbors, it omits stage (b) and is regarded as a straggler in stage (a). For $m' = m$, there is no transmission and thus no outages. The distant PS requires significantly higher power than devices to achieve reliable communication, and thus cannot decode messages from devices at this stage.

(b) *Device-to-PS Communication*: The non-straggler devices from stage (a) encode partial sums $\mathbf{s}_{m,t}$ s to $I_{m,t}^b$ s and transmit $I_{m,t}^b$ s to PS with SNR_b . The link from device m to PS may suffer disruption w.p. P_e^b given in II-B. Then PS decodes $\mathbf{s}_{m,t}$ s from $I_{m,t}^b$ s and detects the straggler pattern \mathbf{a}_k as described in II-C. If such \mathbf{a}_k exists, PS combines the received partial sums according to \mathbf{a}_k . In concrete terms, PS computes the global model update as

$$\Delta\theta_t = \sum_{m=1}^M a_{km} \mathbf{s}_{m,t} = \sum_{m=1}^M p_m \mathcal{Q}(\Delta\theta_{m,t}^\tau), \quad (8)$$

where a_{km} is the m -th element in \mathbf{a}_k . Such \mathbf{a}_k exists if the number of total stragglers is no more than s . Then PS updates the global model as

$$\theta_t \leftarrow \theta_{t-1} + \Delta\theta_t. \quad (9)$$

The devices unable to connect to PS are stragglers in stage (b). At the t -th round, our design either recovers the perfect global model or fails, without possibly receiving a distorted global model by partial participation. If the number of total stragglers exceeds s , the global model is not updated at the t -th round. The training stops when the following two conditions are satisfied: (1) the total number of executed training rounds reaches T , and (2) the global model of the last executed round is successfully updated.

Denote the failure probability of global model recovery at PS per round by P_O , our proposed approach is mirrored by the following learning process, based on which we conduct the convergence analysis in IV-B. In the mirror learning process, the number of consecutive training rounds R_r between $r-1$ -th and r -th successful recovery follows a Geometrical distribution, that is, devices perform $R_r\tau$ -step SGD where $R_r \sim \text{Geo}(1 - P_O)$. Training stops at the first time $\sum_{r=1}^n R_r \geq T$, and $T' = \min\{n \in \mathbb{Z} : \sum_{r=1}^n R_r \geq T\}$ is the executed training rounds.

Algorithm 1 A mirror FL process

- 1: **Initialize** $\theta_0 = 0$, $r = 1$, $R_1 = 1$
 - 2: **while** $\sum_{j=1}^r R_j \leq T$ **do**
 - 3: PS broadcasts θ_{r-1}
 - 4: $R_r = k$ w.p. $P_O^{k-1}(1 - P_O)$
 - 5: **for** $m = 1, \dots, M$ **do**
 - 6: device m performs $R_r\tau$ -step SGD ($\theta_{m,r}^0 = \theta_{r-1}$)
 - 7: device m send $\mathcal{Q}(\Delta\theta_{m,r}^{R_r\tau})$ to device m'
 - 8: **if** device m can compute $s_{m,r}$ in Eq. 7 **then**
 - 9: device m transmits $s_{m,r}$ to PS
 - 10: **end if**
 - 11: **end for**
 - 12: PS computes $\Delta\theta_r$ in Eq.8 and updates θ_r in Eq.9
 - 13: $r = r + 1$
 - 14: **end while**
-

IV. PERFORMANCE ANALYSIS

A. Outage analysis

We first distinguish two types of outages: *i*) the transmission outage, which refers to single link disruption and is modeled in II-B; *ii*) the overall outage, which occurs when GC is dysfunctional. This section focuses on analyzing the type *ii*) outage based on the type *i*) outage. To this end, let us consider the following three sub-cases of the overall outage. For simplicity, assume $\text{SNR}_b = \frac{\beta_a^2}{\beta_b^2} \text{SNR}_a$ such that $P_e^a = P_e^b = P_e$.

1) *No straggler in stage (a)*: Assume no straggler occurs in stage (*a*), i.e., every device successfully recovers s updates of its neighbors. This event occurs w.p. $((1 - P_e)^s)^M$. The overall outage happens when $v_1 \geq s + 1$ device-to-PS links are down, so the overall outage probability in this sub-case is

$$P_1 = (1 - P_e)^{sM} \sum_{v=s+1}^M \binom{M}{v_1} P_e^{v_1} (1 - P_e)^{M-v_1}. \quad (10)$$

2) $v_1 \geq s + 1$ *stragglers in stage (a)*: If there are $v_1 \geq s + 1$ stragglers in stage (*a*), the overall outage happens for sure regardless of the device-to-PS link condition. A device in stage (*a*) is a straggler if at least 1 link between the device and its neighbors is down. The probability of a device being a straggler is $1 - (1 - P_e)^s$. The overall outage probability is

$$P_2 = \sum_{v=s+1}^M \binom{M}{v} (1 - (1 - P_e)^s)^v ((1 - P_e)^s)^{M-v}. \quad (11)$$

3) $1 \sim s$ *stragglers in stage (a)*: Suppose that there are $v_1 \in [s]$ stragglers in stage (*a*), the GC scheme is dysfunctional if there are $v_2 \geq s - v_1 + 1$ stragglers among $M - v_1$ devices in stage (*b*). Thus, the overall outage probability is given by

$$P_3 = \sum_{v_1=1}^s \binom{M}{v_1} (1 - (1 - P_e)^s)^{v_1} ((1 - P_e)^s)^{M-v_1} \cdot \sum_{v_2=s-v_1+1}^{M-v_1} \binom{M-v_1}{v_2} P_e^{v_2} (1 - P_e)^{M-v_1-v_2}. \quad (12)$$

Since sub-cases 1), 2), 3) are non-overlapping, P_O is given by

$$P_O = P_1 + P_2 + P_3. \quad (13)$$

B. Convergence Analysis for Non-convex objective functions

We conduct a non-convex convergence analysis for the proposed scheme with the following assumptions [16] [7] [17].

- A.1 Each local objective function is bounded by $F_m(x) \geq F^*$ and is differentiable, its gradient $\nabla F_m(x)$ is L -smooth, i.e., $\|\nabla F_m(x) - \nabla F_m(y)\| \leq L\|x - y\|$, $\forall i \in [M]$.
- A.2 The local stochastic gradient is an unbiased estimation, i.e., $\mathbb{E}_\xi[\nabla F_m(x, \xi)] = \nabla F_m(x)$, and has bounded data variance $\mathbb{E}_\xi[\|\nabla F_m(x, \xi) - \nabla F_m(x)\|^2] \leq \sigma^2$, $\forall i \in [M]$.
- A.3 The dissimilarity between $\nabla F_m(x)$ and $\nabla F(x)$ is bounded, i.e., $\mathbb{E}[\|\nabla F_m(x) - \nabla F(x)\|^2] \leq D_m^2$, $\forall i \in [M]$.

Theorem 1. *Under A.1~A.3, for a given number of τ iterations on device $m \in [M]$, by adopting the proposed method in which the probability of unsuccessful recovery of the global model is P_O , if the preliminary training rounds T is chosen such that the learning rate $\eta = \frac{1}{L}\sqrt{\frac{M}{T}}$ is small enough, it yields that the proposed algorithm converges w.p. $p \rightarrow 1$.*

$$\begin{aligned}
& \min_{r \in [T']} \mathbb{E} \left[\|\nabla F(\boldsymbol{\theta}_r^0)\|^2 \right] \leq 2(1 - P_O) \cdot \\
& \left\{ \mathcal{O} \left(\frac{1}{1 - P_O} \frac{L(F^* - F(\boldsymbol{\theta}_r^0))}{\sqrt{MT}\tau} \right) \right. \\
& + \mathcal{O} \left(\left(\frac{2\tau(1 + P_O)}{(1 - P_O)^2} \sqrt{\frac{M}{T}} + \frac{MC_1}{L^2T} \right) \sum_{m=1}^M p_m D_m^2 \right) \\
& + \mathcal{O} \left(\left(\frac{\sum_{m=1}^M p_m^2}{2(1 - P_O)} \sqrt{\frac{M}{T}} + \frac{MC_2}{L^2T} \right) \sigma^2 \right) \\
& \left. + \mathcal{O} \left(\frac{1}{2\tau} \sqrt{\frac{M}{T}} \frac{\sum_{r \in [(1 - P_O)T]} \sum_{m=1}^M p_m^2 J_{m,r}^2}{(1 - P_O)T} \right) \right\} \quad (14)
\end{aligned}$$

Remark 1. *Theorem 1 can be easily extended to patch SGD with b nodes by replacing σ^2 by σ^2/b [16].*

V. SIMULATION

In the simulation, the number of devices is set to $M = 10$. Each device employs SQ with 2^8 quantization levels and boundary values of SQ remains the same each round. We run experiments on the MNIST dataset, distribute an equal amount of data to each device, and evaluate the performance of the following four methods under different settings choosing $\beta_a = 1$, $\beta_b = 0.2$,

$\text{SNR}_b = \frac{\beta_a^2}{\beta_b^2} \text{SNR}_a$, i.e., $P_e^a = P_e^b = P_e$. For ease of reading, from now on we adopt SNR to represent SNR_a .

- (i) Quantized FL (QFL) employing digital/analog transmission with perfect links [7], i.e., when $\text{SNR} = \infty$.
- (ii) Our proposed method employing digital transmission, i.e., FL GC with P_e under $\text{SNR} = 3/5$ per device and transmission rate $R = 0.2$.
- (iii) Non-blind FL employing digital transmission [9] with P_e in (ii). The updating rule of $\Delta\theta_t$ follows Eq. 4 in [9].
- (iv) Blind FL with P_e in (ii) [10], which refers to the scenarios where the PS is unaware of the identity of received devices, such as amplify-and-forward.

The preliminary number of training rounds is set to $T = 20$, the number of local iterations $\tau = 5$, the patch size per iteration is set to $|\xi_{m,r}^i| = 1024$ and the learning rate is set to $\eta = 0.01$. The classifier model is implemented using a 4-layer convolutional neural network (CNN) with SGD optimizer that consists of two convolution layers with 10 and 20 output channels respectively followed by 2 fully connected layers. The dimension of learning parameter $d > 10^4$.

The outage probability P_e of individual links and the overall outage probability P_O in terms of SNR are plotted in Fig. 2. From Fig. 2, it is foreseeable that the prevalence of stragglers in low SNR scenarios is higher compared to high SNR scenarios, attributed to an elevated P_e . P_O decreases with increased SNR and s , which indicates that s can be set smaller with larger SNR, and vice versa. In our simulation, s is set to 5 for $\text{SNR} = 5$, and 7 for $\text{SNR} = 3$.

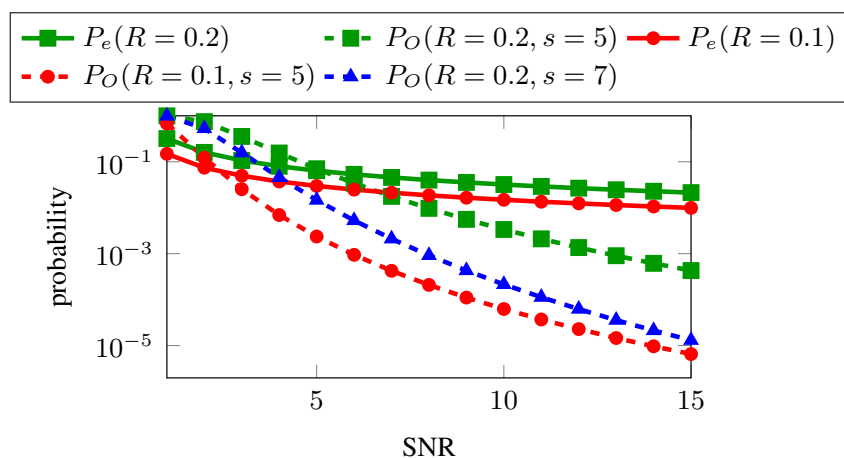


Fig. 2: Outage probability of an individual link and overall outage probability in terms of SNR under different rates

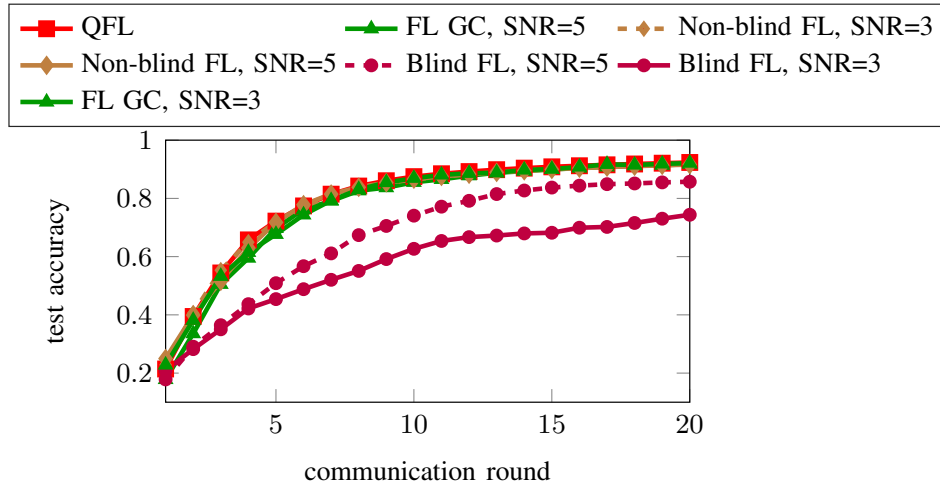


Fig. 3: Test accuracy comparison of four methods under different SNRs in terms of communication round under i.i.d. data distribution.

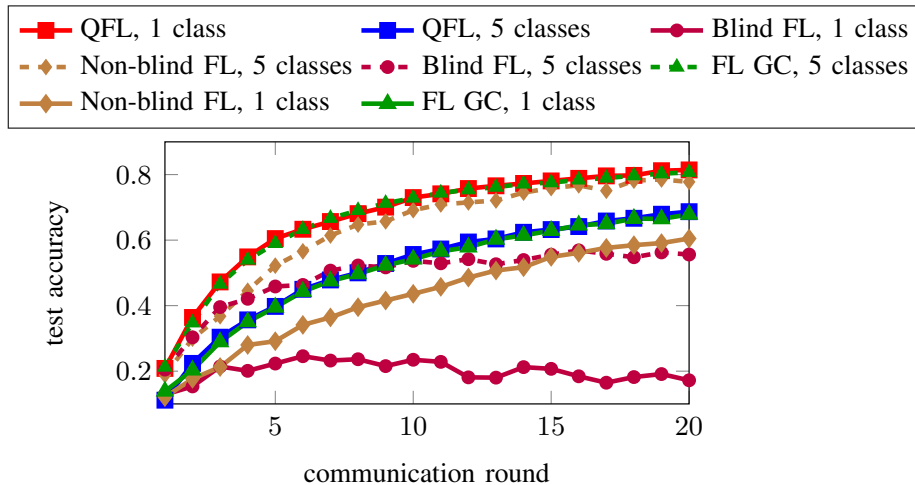


Fig. 4: Test accuracy comparison of four methods under different data imbalances in terms of communication round under non-i.i.d. data distribution.

The average test accuracy of the global model over multiple runs at each round is plotted in Fig. 3 and Fig. 4 for i.i.d case and non-i.i.d. case, respectively. Under i.i.d data distribution, the training samples are shuffled and uniformly assigned to $M = 10$ devices. Under non-i.i.d. data distribution, each device is assigned 5 classes of data and 1 class of data respectively to achieve different extents of data imbalance. To ensure an equitable comparison, we truncate the outcome at 20 rounds. From Fig. 3, we observe that under i.i.d. data distribution, the performance of blind QFL deteriorates with decreased SNR due to more frequent stragglers. The non-blind FL performs well in the presence of stragglers due to homogeneous data distribution across devices.

However, with the increasing data imbalance, as shown in Fig. 4, the non-blind QFL shows a slower convergence and larger generalization gap. The performance of blind FL degrades significantly with more severe data imbalance across devices. In both i.i.d. and non-i.i.d. cases, our proposed algorithm effectively handles stragglers and almost achieves the same performance as the ideal scenarios with infinite SNR.

VI. CONCLUSION

In this paper, we proposed a cooperative GC strategy that achieves GC by cooperative communication to address stragglers in FL. Subsequently, we conducted the convergence analysis based on the outage analysis. Finally, we verified the effectiveness of the proposed strategy by simulation.

REFERENCES

- [1] S. Niknam, H. S. Dhillon, and J. H. Reed, "Federated learning for wireless communications: Motivation, opportunities, and challenges," *IEEE Communications Magazine*, vol. 58, no. 6, pp. 46–51, 2020.
- [2] C. Zhang, Y. Xie, H. Bai, B. Yu, W. Li, and Y. Gao, "A survey on federated learning," *Knowledge-Based Systems*, vol. 216, p. 106775, 2021.
- [3] P. Kairouz, H. B. McMahan, B. Avent, A. Bellet, M. Bennis, A. N. Bhagoji, K. Bonawitz, Z. Charles, G. Cormode, R. Cummings *et al.*, "Advances and open problems in federated learning," *Foundations and Trends® in Machine Learning*, vol. 14, no. 1–2, pp. 1–210, 2021.
- [4] C. T. Dinh, N. H. Tran, M. N. H. Nguyen, C. S. Hong, W. Bao, A. Y. Zomaya, and V. Gramoli, "Federated learning over wireless networks: Convergence analysis and resource allocation," *IEEE/ACM Transactions on Networking*, vol. 29, no. 1, pp. 398–409, 2021.
- [5] M. Xhemrishi, A. G. i Amat, E. Rosnes, and A. Wachter-Zeh, "Computational code-based privacy in coded federated learning," in *2022 IEEE International Symposium on Information Theory (ISIT)*. IEEE, 2022, pp. 2034–2039.
- [6] M. M. Amiri, D. Gunduz, S. R. Kulkarni, and H. V. Poor, "Federated learning with quantized global model updates," 2020.
- [7] M. M. Amiri, D. Gündüz, S. R. Kulkarni, and H. V. Poor, "Convergence of federated learning over a noisy downlink," *IEEE Transactions on Wireless Communications*, vol. 21, no. 3, pp. 1422–1437, 2022.
- [8] H. Xing, O. Simeone, and S. Bi, "Federated learning over wireless device-to-device networks: Algorithms and convergence analysis," *IEEE Journal on Selected Areas in Communications*, vol. 39, no. 12, pp. 3723–3741, 2021.
- [9] Y. Wang, Y. Xu, Q. Shi, and T.-H. Chang, "Quantized federated learning under transmission delay and outage constraints," *IEEE Journal on Selected Areas in Communications*, vol. 40, no. 1, pp. 323–341, 2021.
- [10] R. Saha, M. Yemini, E. Ozfatura, D. Gunduz, and A. Goldsmith, "Colrel: Collaborative relaying for federated learning over intermittently connected networks," in *Workshop on Federated Learning: Recent Advances and New Challenges (in Conjunction with NeurIPS 2022)*, 2022.
- [11] M. Chen, H. V. Poor, W. Saad, and S. Cui, "Wireless communications for collaborative federated learning," *IEEE Communications Magazine*, vol. 58, no. 12, pp. 48–54, 2020.

- [12] R. Schlegel, S. Kumar, E. Rosnes, and A. G. i Amat, “Codedpaddedfl and codedsecagg: Straggler mitigation and secure aggregation in federated learning,” *IEEE Transactions on Communications*, 2023.
- [13] B. McMahan, E. Moore, D. Ramage, S. Hampson, and B. A. y Arcas, “Communication-efficient learning of deep networks from decentralized data,” in *Artificial intelligence and statistics*. PMLR, 2017, pp. 1273–1282.
- [14] M. Xiao and M. Skoglund, “Multiple-user cooperative communications based on linear network coding,” *IEEE Transactions on Communications*, vol. 58, no. 12, pp. 3345–3351, 2010.
- [15] R. Tandon, Q. Lei, A. G. Dimakis, and N. Karampatziakis, “Gradient coding: Avoiding stragglers in distributed learning,” in *International Conference on Machine Learning*. PMLR, 2017, pp. 3368–3376.
- [16] X. Lian, C. Zhang, H. Zhang, C.-J. Hsieh, W. Zhang, and J. Liu, “Can decentralized algorithms outperform centralized algorithms? a case study for decentralized parallel stochastic gradient descent,” *Advances in neural information processing systems*, vol. 30, 2017.
- [17] J. Wang, Q. Liu, H. Liang, G. Joshi, and H. V. Poor, “Tackling the objective inconsistency problem in heterogeneous federated optimization,” *Advances in neural information processing systems*, vol. 33, pp. 7611–7623, 2020.
- [18] Y. Wang, Y. Xu, Q. Shi, and T.-H. Chang, “Quantized federated learning under transmission delay and outage constraints,” *IEEE Journal on Selected Areas in Communications*, vol. 40, no. 1, p. 323–341, Jan. 2022. [Online]. Available: <http://dx.doi.org/10.1109/JSAC.2021.3126081>

APPENDIX A

PROOF OF THEOREM 1

Proof. Assume that the $R_r - 1$ overall outages happen before r -th round successful aggregation, that is, edge devices perform $R_r\tau$ -step consecutive SGD before the successful aggregation during the r -th round. According to A.1, it holds that

$$\mathbb{E} [F(\boldsymbol{\theta}_{r+1}^0)] - \mathbb{E} [F(\boldsymbol{\theta}_r^0)] \stackrel{\text{A.1}}{\leq} \mathbb{E} [\langle \nabla F(\boldsymbol{\theta}_r^0), \boldsymbol{\theta}_{r+1}^0 - \boldsymbol{\theta}_r^0 \rangle] + \frac{L}{2} \mathbb{E} [\|\boldsymbol{\theta}_{r+1}^0 - \boldsymbol{\theta}_r^0\|^2]. \quad (15)$$

Next we complete the proof of Theorem 1 with the help of the following lemmas.

Lemma 1. *The properties of stochastic quantization have been established in [18], for ease of reference, we fit it in our case.*

$$\mathbb{E} [\mathcal{Q}(\Delta\boldsymbol{\theta}_{m,r})] = \Delta\boldsymbol{\theta}_{m,r} \quad (16)$$

$$\mathbb{E} [\|\mathcal{Q}(\Delta\boldsymbol{\theta}_{m,r}) - \Delta\boldsymbol{\theta}_{m,r}\|^2] \leq \frac{\eta^2 \delta_{m,r}^2}{(2^{B_{m,r}} - 1)^2} \triangleq \eta^2 J_{m,r}^2 \quad (17)$$

where $\delta_{m,r} \triangleq \sqrt{\frac{1}{4} \sum_{j=1}^d (\nabla F_{m,r} - \nabla F_{m,r})^2}$ by defining $\nabla F_{m,r} = \sum_{i=0}^{R_r\tau-1} \nabla F_m(\boldsymbol{\theta}_{m,r}^i, \boldsymbol{\xi}_{m,r}^i)$.

Lemma 2. *Under A.1~A.3, it holds that*

$$\mathbb{E} [\langle \nabla F(\boldsymbol{\theta}_r^0), \boldsymbol{\theta}_{r+1}^0 - \boldsymbol{\theta}_r^0 \rangle] \leq -\frac{1}{2} \eta R_r \tau \mathbb{E} [\|\nabla F(\boldsymbol{\theta}_r^0)\|^2] + \frac{1}{2} \eta L^2 \sum_{i=0}^{R_r\tau-1} \sum_{m=1}^M p_m \mathbb{E} [\|\boldsymbol{\theta}_{m,r}^0 - \boldsymbol{\theta}_{m,r}^i\|^2] \quad (18)$$

Proof. L.2 is proved in Appendix B. \square

Lemma 3. *Under A.1~A.3, it holds that*

$$\begin{aligned} \mathbb{E} [\|\boldsymbol{\theta}_{r+1}^0 - \boldsymbol{\theta}_r^0\|^2] &\leq \eta^2 \sum_{m=1}^M p_m^2 J_{m,r}^2 + \eta^2 R_r \tau \sigma^2 \sum_{m=1}^M p_m^2 + 2\eta^2 R_r \tau \sum_{m=1}^M p_m \sum_{i=0}^{R_r \tau - 1} L^2 \mathbb{E} [\|\boldsymbol{\theta}_{m,r}^i - \boldsymbol{\theta}_r^0\|^2] \\ &\quad + 4\eta^2 R_r^2 \tau^2 \sum_{m=1}^M p_m D_m^2 + 4\eta^2 R_r^2 \tau^2 \mathbb{E} [\|\nabla F(\boldsymbol{\theta}_r^0)\|^2], \end{aligned} \quad (19)$$

Proof. L.3 is proved in Appendix C. \square

Lemma 4. *Under A.1~A.3, it holds that*

$$\begin{aligned} \sum_{i=0}^{R_r \tau - 1} \mathbb{E} [\|\boldsymbol{\theta}_{m,r}^i - \boldsymbol{\theta}_{m,r}^0\|^2] &\leq \frac{\frac{1}{2} R_r \tau (R_r \tau + 1)}{1 - R_r \tau (R_r \tau + 1) \eta^2 L^2} \eta^2 \sigma^2 + \frac{\frac{2}{3} R_r \tau (R_r \tau + 1) (2R_r \tau + 1)}{1 - R_r \tau (R_r \tau + 1) \eta^2 L^2} \eta^2 D_m^2 \\ &\quad + \frac{\frac{2}{3} R_r \tau (R_r \tau + 1) (2R_r \tau + 1)}{1 - R_r \tau (R_r \tau + 1) \eta^2 L^2} \eta^2 \mathbb{E} [\|\nabla F(\boldsymbol{\theta}_r^0)\|^2]. \end{aligned} \quad (20)$$

Proof. L.4 is proved in Appendix D. \square

By substituting L.2 and L.3 into for into Eq.15, we obtain the immediate result as follows.

$$\begin{aligned} \mathbb{E}[F(\boldsymbol{\theta}_{r+1}^0)] - \mathbb{E}[F(\boldsymbol{\theta}_r^0)] &\leq \left(2\eta^2 R_r^2 \tau^2 L - \frac{1}{2} \eta R_r \tau \right) \mathbb{E} [\|\nabla F(\boldsymbol{\theta}_r^0)\|^2] + 2\eta^2 R_r^2 \tau^2 L \sum_{m=1}^M p_m D_m^2 \\ &\quad + \left(\frac{1}{2} \eta L^2 + \eta^2 L^3 R_r \tau \right) \sum_{m=1}^M p_m \sum_{i=0}^{R_r \tau - 1} \mathbb{E} [\|\boldsymbol{\theta}_{m,r}^i - \boldsymbol{\theta}_r^0\|^2] + \frac{1}{2} \eta^2 L \sum_{m=1}^M p_m^2 J_{m,r}^2 + \frac{1}{2} \eta^2 L R_r \tau \sigma^2 \sum_{m=1}^M p_m^2 \end{aligned} \quad (21)$$

Utilize results from L.4, re-arrange the terms, divide both sides by $\eta\tau$, and average over the executed T' rounds, we obtain

$$\begin{aligned} \frac{1}{T'} \sum_{r \in [T']} H_1 \mathbb{E} [\|\nabla F(\boldsymbol{\theta}_r^0)\|^2] &\leq \frac{1}{T'} H_2 (F^* - F(\boldsymbol{\theta}_r^0)) + \frac{1}{T'} \sum_{r \in [T']} H_3 \sum_{m=1}^M p_m D_m^2 \\ &\quad + \frac{1}{T'} \sum_{r \in [T']} H_4 \sigma^2 + \frac{1}{T'} \sum_{r \in [T']} H_5 \sum_{m=1}^M p_m^2 J_{m,r}^2, \end{aligned} \quad (22)$$

where

$$\begin{aligned} H_1 &= \frac{1}{2} R_r - H_3, \quad H_2 = \frac{1}{\eta\tau}, \quad H_5 = \frac{\eta L}{2\tau}, \\ H_3 &= 2\eta R_r^2 \tau L + \eta^2 \underbrace{\frac{\frac{2}{3} L^2 R_r (R_r \tau + 1) (2R_r \tau + 1) (\frac{1}{2} + \eta R_r \tau L)}{1 - R_r \tau (R_r \tau + 1) \eta^2 L^2}}_{c_1}, \end{aligned}$$

$$H_4 = \frac{1}{2}\eta R_r L \sum_{m=1}^M p_m^2 + \eta^2 \underbrace{\frac{\frac{1}{2}L^2 R_r (R_r \tau + 1)(\frac{1}{2} + \eta R_r \tau L)}{1 - R_r \tau (R_r \tau + 1)\eta^2 L^2}}_{c_2}.$$

By ratio test in Eq.24, we verify $\mathbb{E}[c_1]$ converges to finite C_1 .

$$\mathbb{E}[c_1] = \sum_{R_r=1}^{\infty} c_1 \underbrace{(1 - P_O) P_O^{R_r - 1}}_{c_3(R_r)} \quad (23)$$

$$\lim_{R_r \rightarrow \infty} \frac{c_3(R_r + 1)}{c_3(R_r)} = P_O < 1 \quad (24)$$

Similarly, we can verify $\mathbb{E}[c_2]$ converges to finite C_2 .

Since R_r follows geometrical distribution, it can be shown that $\mathbb{E}[R_r] = \frac{1}{1 - P_O}$ and $\mathbb{E}[R_r^2] = \frac{1 + P_O}{(1 - P_O)^2}$. Subsequently,

$$\mathbb{E}[H_3] = 2\eta\tau L \frac{1 + P_O}{(1 - P_O)^2} + \eta^2 C_1,$$

$$\mathbb{E}[H_4] = \frac{1}{2}\eta L \sum_{m=1}^M p_m^2 \frac{1}{1 - P_O} + \eta^2 C_2,$$

$$\mathbb{E}[H_1] = \frac{1}{2(1 - P_O)} - \mathbb{E}[H_3]$$

When $T \rightarrow \infty$, R_r are i.i.d. geometrical variables, By L.2 and law of large numbers $T' = \left\lceil \frac{T}{\mathbb{E}[R_r]} \right\rceil \approx (1 - P_O)T$ w.p. $p \rightarrow 1$. When $P_O \ll 1$, Eq.22 can be approximated as

$$\begin{aligned} \mathbb{E}[H_1] \min_{r \in [(1 - P_O)T]} \mathbb{E} \left[\|\nabla F(\boldsymbol{\theta}_r^0)\|^2 \right] &\leq \frac{H_2}{(1 - P_O)T} (F^* - F(\boldsymbol{\theta}_r^0)) + \mathbb{E}[H_3] \sum_{m=1}^M p_m D_m^2 \\ &+ \mathbb{E}[H_4] \sigma^2 + \frac{H_5}{(1 - P_O)T} \sum_{r \in [(1 - P_O)T]} \sum_{m=1}^M p_m^2 J_{m,r}^2. \end{aligned} \quad (25)$$

By choosing learning rate $\eta = \frac{1}{L} \sqrt{\frac{M}{T}}$, we complete the proof. \square

APPENDIX B

PROOF OF LEMMA 2

The term $\mathbb{E} \left[\langle \nabla F(\boldsymbol{\theta}_r^0), \boldsymbol{\theta}_{r+1}^0 - \boldsymbol{\theta}_r^0 \rangle \right]$ is bounded by

$$\begin{aligned} &\mathbb{E} \left[\langle \nabla F(\boldsymbol{\theta}_r^0), \boldsymbol{\theta}_{r+1}^0 - \boldsymbol{\theta}_r^0 \rangle \right] \\ &= \mathbb{E} \left[\left\langle \nabla F(\boldsymbol{\theta}_r^0), \sum_{j=1}^M a_{kj} \sum_{m=1}^M b_{jm} p_m \mathcal{Q}(\Delta \boldsymbol{\theta}_{r,m}^{R_r \tau - 1}) \right\rangle \right] \end{aligned}$$

$$\begin{aligned}
&\stackrel{\text{L.1}}{=} -\eta \mathbb{E} \left[\left\langle \nabla F(\boldsymbol{\theta}_r^0), \sum_{m=1}^M p_m \sum_{i=0}^{R_r\tau-1} \nabla F_m(\boldsymbol{\theta}_{m,r}^i, \boldsymbol{\xi}_{m,r}^i) \right\rangle \right] \\
&\stackrel{\text{(a)}}{=} -\eta \sum_{i=0}^{R_r\tau-1} \mathbb{E} \left[\left\langle \nabla F(\boldsymbol{\theta}_r^0), \sum_{m=1}^M p_m \nabla F_m(\boldsymbol{\theta}_{m,r}^i) \right\rangle \right] \\
&\stackrel{\text{(b)}}{=} -\frac{1}{2}\eta \sum_{i=0}^{R_r\tau-1} \mathbb{E} \left[\|\nabla F(\boldsymbol{\theta}_r^0)\|^2 \right] - \frac{1}{2}\eta \sum_{i=0}^{R_r\tau-1} \mathbb{E} \left[\left\| \sum_{m=1}^M p_m \nabla F_m(\boldsymbol{\theta}_{m,r}^i) \right\|^2 \right] \\
&\quad + \frac{1}{2}\eta \sum_{i=0}^{R_r\tau-1} \mathbb{E} \left[\left\| \nabla F(\boldsymbol{\theta}_r^0) - \sum_{m=1}^M p_m \nabla F_m(\boldsymbol{\theta}_{m,r}^i) \right\|^2 \right] \\
&\stackrel{\text{(c)}}{\leq} -\frac{1}{2}\eta R_r\tau \mathbb{E} \left[\|\nabla F(\boldsymbol{\theta}_r^0)\|^2 \right] + \frac{1}{2}\eta \sum_{i=0}^{R_r\tau-1} \sum_{m=1}^M p_m \mathbb{E} \left[\|\nabla F_m(\boldsymbol{\theta}_r^0) - \nabla F_m(\boldsymbol{\theta}_{m,r}^i)\|^2 \right] \\
&\stackrel{\text{A.1}}{\leq} -\frac{1}{2}\eta R_r\tau \mathbb{E} \left[\|\nabla F(\boldsymbol{\theta}_r^0)\|^2 \right] + \frac{1}{2}\eta L^2 \sum_{i=0}^{R_r\tau-1} \sum_{m=1}^M p_m \mathbb{E} \left[\|\boldsymbol{\theta}_{m,r}^0 - \boldsymbol{\theta}_{m,r}^i\|^2 \right] \tag{26}
\end{aligned}$$

where (a) follows A.2 and property of inner product, (b) follows the fact that $\langle a, b \rangle = \frac{1}{2}\|a\|^2 + \frac{1}{2}\|b\|^2 - \frac{1}{2}\|a - b\|^2$, (c) follows $\nabla F(\boldsymbol{\theta}_r^0) = \sum_{m=1}^M p_m \nabla F_m(\boldsymbol{\theta}_r^0)$ and the convexity of l_2 -norm.

APPENDIX C

PROOF OF LEMMA 3

The term $\mathbb{E} [\|\boldsymbol{\theta}_{r+1}^0 - \boldsymbol{\theta}_r^0\|^2]$ is bounded by

$$\begin{aligned}
\mathbb{E} [\|\boldsymbol{\theta}_{r+1}^0 - \boldsymbol{\theta}_r^0\|^2] &= \mathbb{E} \left[\left\| \sum_{m=1}^M p_m \mathcal{Q}(\Delta\boldsymbol{\theta}_{r,m}^{R_r\tau-1}) \right\|^2 \right] \\
&\stackrel{\text{(d)}}{=} \mathbb{E} \left[\left\| \sum_{m=1}^M p_m (\mathcal{Q}(\Delta\boldsymbol{\theta}_{r,m}^{R_r\tau-1}) - \Delta\boldsymbol{\theta}_{r,m}^{R_r\tau-1}) \right\|^2 \right] + \mathbb{E} \left[\left\| \sum_{m=1}^M p_m \Delta\boldsymbol{\theta}_{r,m}^{R_r\tau-1} \right\|^2 \right] \\
&\stackrel{\text{(e)}}{=} \sum_{m=1}^M p_m^2 \mathbb{E} \left[\left\| \mathcal{Q}(\Delta\boldsymbol{\theta}_{r,m}^{R_r\tau-1}) - \Delta\boldsymbol{\theta}_{r,m}^{R_r\tau-1} \right\|^2 \right] + \eta^2 \mathbb{E} \left[\left\| \sum_{m=1}^M p_m \sum_{i=0}^{R_r\tau-1} \nabla F_m(\boldsymbol{\theta}_{m,r}^i, \boldsymbol{\xi}_{m,r}^i) \right\|^2 \right] \\
&\stackrel{\text{(f)}}{=} \sum_{m=1}^M p_m^2 J_{m,r}^2 + \eta^2 \mathbb{E} \left[\left\| \sum_{m=1}^M p_m \sum_{i=0}^{R_r\tau-1} \nabla F_m(\boldsymbol{\theta}_{m,r}^i) \right\|^2 \right] \\
&\quad + \eta^2 \mathbb{E} \left[\left\| \sum_{m=1}^M p_m \sum_{i=0}^{R_r\tau-1} (\nabla F_m(\boldsymbol{\theta}_{m,r}^i, \boldsymbol{\xi}_{m,r}^i) - \nabla F_m(\boldsymbol{\theta}_{m,r}^i)) \right\|^2 \right] \\
&\stackrel{\text{(g)}}{=} \sum_{m=1}^M p_m^2 J_{m,r}^2 + \eta^2 \mathbb{E} \left[\left\| \sum_{m=1}^M p_m \sum_{i=0}^{R_r\tau-1} \nabla F_m(\boldsymbol{\theta}_{m,r}^i) \right\|^2 \right]
\end{aligned}$$

$$\begin{aligned}
& + \eta^2 \sum_{m=1}^M p_m^2 \sum_{i=0}^{R_r \tau - 1} \mathbb{E} \left[\left\| (\nabla F_m(\boldsymbol{\theta}_{m,r}^i, \boldsymbol{\xi}_{m,r}^i) - \nabla F_m(\boldsymbol{\theta}_{m,r}^i)) \right\|^2 \right] \\
& \stackrel{\text{A.2}}{\leq} \sum_{m=1}^M p_m^2 J_{m,r}^2 + \eta^2 R_r \tau \sigma^2 \sum_{m=1}^M p_m^2 + \eta^2 \sum_{m=1}^M p_m \mathbb{E} \left[\left\| \sum_{i=0}^{R_r \tau - 1} \nabla F_m(\boldsymbol{\theta}_{m,r}^i) - \nabla F_m(\boldsymbol{\theta}_{m,r}^0) + \nabla F_m(\boldsymbol{\theta}_{m,r}^0) \right\|^2 \right] \\
& \stackrel{\text{(h)}}{\leq} \sum_{m=1}^M p_m^2 J_{m,r}^2 + \eta^2 R_r \tau \sigma^2 \sum_{m=1}^M p_m^2 + 2\eta^2 \sum_{m=1}^M p_m \mathbb{E} \left[\left\| \sum_{i=0}^{R_r \tau - 1} \nabla F_m(\boldsymbol{\theta}_{m,r}^i) - \nabla F_m(\boldsymbol{\theta}_r^0) \right\|^2 \right] \\
& \quad + 2\eta^2 \sum_{m=1}^M p_m \mathbb{E} \left[\left\| \sum_{i=0}^{R_r \tau - 1} \nabla F_m(\boldsymbol{\theta}_r^0) \right\|^2 \right] \\
& \stackrel{\text{A.1}}{\leq} \sum_{m=1}^M p_m^2 J_{m,r}^2 + \eta^2 R_r \tau \sigma^2 \sum_{m=1}^M p_m^2 + 2\eta^2 R_r \tau \sum_{m=1}^M p_m \sum_{i=0}^{R_r \tau - 1} L^2 \mathbb{E} \left[\|\boldsymbol{\theta}_{m,r}^i - \boldsymbol{\theta}_r^0\|^2 \right] \\
& \quad + 2\eta^2 R_r^2 \tau^2 \sum_{m=1}^M p_m \mathbb{E} \left[\|\nabla F_m(\boldsymbol{\theta}_r^0) - F(\boldsymbol{\theta}_r^0) + F(\boldsymbol{\theta}_r^0)\|^2 \right] \\
& \stackrel{\text{(i)}}{\leq} \sum_{m=1}^M p_m^2 J_{m,r}^2 + \eta^2 R_r \tau \sigma^2 \sum_{m=1}^M p_m^2 + 2\eta^2 L^2 R_r \tau \sum_{m=1}^M p_m \sum_{i=0}^{R_r \tau - 1} \mathbb{E} \left[\|\boldsymbol{\theta}_{m,r}^i - \boldsymbol{\theta}_r^0\|^2 \right] \\
& \quad + 4\eta^2 R_r^2 \tau^2 \sum_{m=1}^M p_m \mathbb{E} \left[\|\nabla F_m(\boldsymbol{\theta}_r^0) - F(\boldsymbol{\theta}_r^0)\|^2 \right] + 4\eta^2 R_r^2 \tau^2 \sum_{m=1}^M p_m \mathbb{E} \left[\|\nabla F(\boldsymbol{\theta}_r^0)\|^2 \right] \\
& \stackrel{\text{(j)}}{\leq} \eta^2 \sum_{m=1}^M p_m^2 J_{m,r}^2 + \eta^2 R_r \tau \sigma^2 \sum_{m=1}^M p_m^2 + 2\eta^2 R_r \tau \sum_{m=1}^M p_m \sum_{i=0}^{R_r \tau - 1} L^2 \mathbb{E} \left[\|\boldsymbol{\theta}_{m,r}^i - \boldsymbol{\theta}_r^0\|^2 \right] \\
& \quad + 4\eta^2 R_r^2 \tau^2 \sum_{m=1}^M p_m D_m^2 + 4\eta^2 R_r^2 \tau^2 \mathbb{E} \left[\|\nabla F(\boldsymbol{\theta}_r^0)\|^2 \right], \tag{27}
\end{aligned}$$

where the equality (d), (f) follows the fact that $\mathbb{E}[\|x\|^2] = \|\mathbb{E}[x]\|^2 + \mathbb{E}[\|x - \mathbb{E}[x]\|^2]$, the equality (e), (g) is due to unbiased estimation and lemma 2 in [17], (h), (i) follows the fact that $\|a+b\|^2 \leq 2\|a\|^2 + 2\|b\|^2$, (j) follows A.3 and L.1.

APPENDIX D

PROOF OF LEMMA 4

Proof 1.

$$\begin{aligned}
\mathbb{E} \left[\|\boldsymbol{\theta}_{m,r}^0 - \boldsymbol{\theta}_{m,r}^i\|^2 \right] & = \eta^2 \mathbb{E} \left[\left\| \sum_{s=0}^{i-1} \nabla F_m(\boldsymbol{\theta}_{m,r}^s, \boldsymbol{\xi}_{m,r}^s) \right\|^2 \right] \\
& \stackrel{\text{(k)}}{=} \eta^2 \mathbb{E} \left[\left\| \sum_{s=0}^{i-1} (\nabla F_m(\boldsymbol{\theta}_{m,r}^s, \boldsymbol{\xi}_{m,r}^s) - \nabla F_m(\boldsymbol{\theta}_{m,r}^s)) \right\|^2 \right] + \eta^2 \mathbb{E} \left[\left\| \sum_{s=0}^{i-1} \nabla F_m(\boldsymbol{\theta}_{m,r}^s) \right\|^2 \right]
\end{aligned}$$

$$\begin{aligned}
&\stackrel{(l)}{=} \eta^2 \sum_{s=0}^{i-1} \mathbb{E} \left[\left\| \nabla F_m(\boldsymbol{\theta}_{m,r}^s, \xi_{m,r}^s) - \nabla F_m(\boldsymbol{\theta}_{m,r}^s) \right\|^2 \right] + \eta^2 \mathbb{E} \left[\left\| \sum_{s=0}^{i-1} \nabla F_m(\boldsymbol{\theta}_{m,r}^s) \right\|^2 \right] \\
&\stackrel{(m)}{\leq} \eta^2 i \sigma^2 + \eta^2 i \sum_{s=0}^{i-1} \mathbb{E} \left[\left\| \nabla F_m(\boldsymbol{\theta}_{m,r}^s) \right\|^2 \right] \\
&= \eta^2 i \sigma^2 + \eta^2 i \sum_{s=0}^{i-1} \mathbb{E} \left[\left\| \nabla F_m(\boldsymbol{\theta}_{m,r}^s) - \nabla F_m(\boldsymbol{\theta}_{m,r}^0) + \nabla F_m(\boldsymbol{\theta}_{m,r}^0) \right\|^2 \right] \\
&\stackrel{(n)}{\leq} \eta^2 i \sigma^2 + 2\eta^2 i \sum_{s=0}^{i-1} \mathbb{E} \left[\left\| \nabla F_m(\boldsymbol{\theta}_{m,r}^s) - \nabla F_m(\boldsymbol{\theta}_{m,r}^0) \right\|^2 \right] \\
&\quad + 2\eta^2 i \sum_{s=0}^{i-1} \mathbb{E} \left[\left\| \nabla F_m(\boldsymbol{\theta}_{m,r}^0) - \nabla F(\boldsymbol{\theta}_r^0) + \nabla F(\boldsymbol{\theta}_r^0) \right\|^2 \right] \\
&\stackrel{A.1}{\leq} \eta^2 i \sigma^2 + 2\eta^2 i L^2 \sum_{s=0}^{i-1} \mathbb{E} \left[\left\| \boldsymbol{\theta}_{m,r}^s - \boldsymbol{\theta}_{m,r}^0 \right\|^2 \right] + 4\eta^2 i \sum_{s=0}^{i-1} \mathbb{E} \left[\left\| \nabla F_m(\boldsymbol{\theta}_{m,r}^0) - \nabla F(\boldsymbol{\theta}_r^0) \right\|^2 \right] \\
&\quad + 4\eta^2 i \sum_{s=0}^{i-1} \mathbb{E} \left[\left\| \nabla F(\boldsymbol{\theta}_r^0) \right\|^2 \right] \\
&\stackrel{(o)}{\leq} \eta^2 i \sigma^2 + 2\eta^2 i L^2 \sum_{s=0}^{i-1} \mathbb{E} \left[\left\| \boldsymbol{\theta}_{m,r}^s - \boldsymbol{\theta}_{m,r}^0 \right\|^2 \right] + 4\eta^2 i^2 D_m^2 + 4\eta^2 i^2 \mathbb{E} \left[\left\| \nabla F(\boldsymbol{\theta}_r^0) \right\|^2 \right], \quad (28)
\end{aligned}$$

where the equality (k) follows $\mathbb{E}[\|x\|^2] = \|\mathbb{E}[x]\|^2 + \mathbb{E}[\|x - \mathbb{E}[x]\|^2]$, (l) is due to unbiased estimation and Lemma 2 in [17], (m) follows A.2, the convexity of l_2 -norm and Jensen's inequality, (n) follows $\|a + b\|^2 \leq 2\|a\|^2 + 2\|b\|^2$, (o) utilizes the fact $\boldsymbol{\theta}_{m,r}^0 = \boldsymbol{\theta}_r^0$ and A.3. \square

Proof 2. Next, we prove the bound for the sum: $\sum_{i=0}^{R_r\tau-1} \mathbb{E} \left[\left\| \boldsymbol{\theta}_{m,r}^0 - \boldsymbol{\theta}_{m,r}^i \right\|^2 \right]$.

$$\begin{aligned}
&\sum_{i=0}^{R_r\tau-1} \mathbb{E} \left[\left\| \boldsymbol{\theta}_{m,r}^0 - \boldsymbol{\theta}_{m,r}^i \right\|^2 \right] \\
&\leq \sum_{i=0}^{R_r\tau-1} \left(\eta^2 i \sigma^2 + 2\eta^2 i L^2 \sum_{s=0}^{i-1} \mathbb{E} \left[\left\| \boldsymbol{\theta}_{m,r}^s - \boldsymbol{\theta}_{m,r}^0 \right\|^2 \right] + 4\eta^2 i^2 D_m^2 + 4\eta^2 i^2 \mathbb{E} \left[\left\| \nabla F(\boldsymbol{\theta}_r^0) \right\|^2 \right] \right) \\
&\stackrel{(p)}{\leq} \frac{1}{2} R_r\tau (R_r\tau + 1) \eta^2 \sigma^2 + \eta^2 L^2 R_r\tau (R_r\tau + 1) \sum_{s=0}^{R_r\tau-1} \mathbb{E} \left[\left\| \boldsymbol{\theta}_{m,r}^s - \boldsymbol{\theta}_{m,r}^0 \right\|^2 \right] \\
&\quad + \frac{2}{3} R_r\tau (R_r\tau + 1) (2R_r\tau + 1) \eta^2 D_m^2 + \frac{2}{3} R_r\tau (R_r\tau + 1) (2R_r\tau + 1) \eta^2 \mathbb{E} \left[\left\| \nabla F(\boldsymbol{\theta}_r^0) \right\|^2 \right], \quad (29)
\end{aligned}$$

where the equality (p) follows that $\sum_{i=1}^n i = \frac{n(n+1)}{2}$, $\sum_{i=1}^n i^2 = \frac{n(n+1)(2n+1)}{6}$, and that $i \leq R_r\tau - 1$. Both sides of Eq.29 contain $\sum_{i=0}^{R_r\tau-1} \mathbb{E} \left[\|\boldsymbol{\theta}_{m,r}^0 - \boldsymbol{\theta}_{m,r}^i\|^2 \right]$, by minor arrangement,

$$\begin{aligned}
& (1 - R_r\tau(R_r\tau + 1)\eta^2 L^2) \sum_{i=0}^{R_r\tau-1} \mathbb{E} \left[\|\boldsymbol{\theta}_{m,r}^0 - \boldsymbol{\theta}_{m,r}^i\|^2 \right] \\
& \leq \frac{1}{2} R_r\tau(R_r\tau + 1)\eta^2 \sigma^2 + \frac{2}{3} R_r\tau(R_r\tau + 1)(2R_r\tau + 1)\eta^2 D_m^2 \\
& \quad + \frac{2}{3} R_r\tau(R_r\tau + 1)(2R_r\tau + 1)\eta^2 \mathbb{E} \left[\|\nabla F(\boldsymbol{\theta}_r^0)\|^2 \right]. \tag{30}
\end{aligned}$$

With $1 - R_r\tau(R_r\tau + 1)\eta^2 L^2 > 0$, we reach the second result in L.4.

□